Identification of a renal-specific oxido-reductase in newborn diabetic mice

Qiwei Yang*, Bharat Dixit†, Jun Wada*, Yufeng Tian*, Elisabeth I. Wallner*, Satish K. Srivastva†, and Yashpal S. Kanwar*‡

*Department of Pathology, Northwestern University Medical School, Chicago, IL 60611; and †Department of Biochemistry, University of Texas Medical Branch, Galveston, TX 77555

Communicated by Emanuel Margoliash, University of Illinois, Chicago, IL, June 8, 2000 (received for review February 23, 2000)

Aldose reductase (ALR2), a NADPH-dependent aldo-keto reductase (AKR), is widely distributed in mammalian tissues and has been implicated in complications of diabetes, including diabetic nephropathy. To identify a renal-specific reductase belonging to the AKR family, representational difference analyses of cDNA from diabetic mouse kidney were performed. A full-length cDNA with an ORF of 855 nt and yielding a ≈1.5-kb mRNA transcript was isolated from a mouse kidney library. Human and rat homologues also were isolated, and they had ≈91% and ≈97% amino acid identity with mouse protein. *In vitro* translation of the cDNA yielded a protein product of ≈33 kDa. Northern and Western blot analyses, using the cDNA and antirecombinant protein antibody, revealed its expression exclusively confined to the kidney. Like ALR2, the expression was up-regulated in diabetic kidneys. Its mRNA and protein expression was restricted to renal proximal tubules. The gene neither codistributed with Tamm–Horsfall protein nor aquaporin-2. The deduced protein sequence revealed an AKR-3 motif located near the N terminus, unlike the other AKR family members where it is confined to the C terminus. Fluorescence quenching and reactive blue agarose chromatography studies revealed that it binds to NADPH with high affinity (K_{dNADPH} = 66.9 ± 2.3 nM). This binding domain is a tetrapeptide (Met-Ala-Lys-Ser) located within the AKR-3 motif that is similar to the other AKR members. The identified protein is designated as RSOR because it is renal-specific with properties of an oxido-reductase, and like ALR2 it may be relevant in the renal complications of diabetes mellitus.

diabetes mellitus | diabetic nephropathy

Renal complications are a common manifestation of diabetes mellitus. Characteristics of these complications are an increase of extracellular matrix (ECM) proteins, i.e., type I and type IV collagens and decorin and fibronectin, synthesized by glomerular, tubular, and interstitial cells (1). The increase in ECM may be multifactorial, but recent studies have narrowed it down to two or three pathogenetic mechanisms that are affected by hyperglycemia. The hyperglycemia may increase the mRNA expression and bioactivity of certain cytokines that modulate the synthesis of various ECM proteins, e.g., transforming growth factor β (2, 3). Nonenzymatic glycation is another mechanism by which various Amadori intermediaries lead to the generation of advanced glycation products (AGEs). The AGEs further cross-link the glycated proteins with one another and render them extremely resistant to proteolytic degradation, resulting in an accumulation of ECM in the kidney (4). Such an AGE-mediated cross-linking process is not restricted to the kidney tissue proteins alone, but it affects other tissue proteins as well, e.g., ocular lens crystallins (5, 6). Another mechanism that is also relevant to diabetic nephropathy is the polyol pathway, which consists of two major reactions. First, glucose is reduced by aldose reductase (ALR2) to sorbitol by using NADPH as the hydrogen donor. The sorbitol then is oxidized by sorbitol dehydrogenase to fructose by using NAD as the hydrogen acceptor (7). Conceivably, there is a link between the polyol pathway and the glycation of collagens and fibronectin by excessive amounts of fructose generated from sorbitol because the synthesis of these ECM proteins can be normalized by the use of an ALR2 inhibitor, sorbinil (8, 9). The linkage of these two pathways also is supported by studies that showed ALR2 to have a high substrate affinity for glycated methylglyoxal (10). Because of the original description of ALR2, a number of aldo-keto reductase (AKR) family members have been discovered in various mammalian tissues (11). So far, among this superfamily, there is no known renal-specific reductase that has been described and can be linked to hyperglycemia in diabetes mellitus. In view of the above considerations, we initiated studies to search for such a reductase, using representational difference analysis (RDA) of cDNA (12), in the kidneys of streptozotocin-induced diabetes in newborn mice. A number of cDNA fragments were isolated that had up-regulated mRNA expression. In this communication, we describe the identification of a kidney-specific oxido-reductase that is up-regulated in the hyperglycemic state.

Materials and Methods

Induction of Diabetes in Newborn Mice. Hyperglycemic state was induced in ICR newborn mice (Harlan) by an i.p. injection of streptozotocin (200 mg/kg of weight) in citrate buffer. Control mice received buffer only. After 3 weeks, kidneys of mice with blood glucose levels >250 mg/dl were harvested and snap-frozen in liquid nitrogen, and total RNA was extracted.

RDA. The method of cDNA-RDA was used to isolate glucose-induced genes in the kidneys of diabetic mice (DM) (12). Briefly, total RNA from normal mouse (NM) and DM kidneys was isolated, poly(A)$^+$ RNA was selected, and first- and second-strand cDNAs were synthesized. The double-stranded cDNAs were subjected to subtractive hybridization, where the NM kidney cDNA was used as the driver and that of the DM kidney as the tester. After three rounds of subtractive hybridization, the difference products (DPs) were isolated and analyzed by 2% agarose gel electrophoresis. After removal of the linkers by digestion with *Dpn*II, they were ligated into *Bam*HI-digested pBluescript KS(+) (Stratagene). After transformation, bacterial colonies were picked to prepare plasmid DNAs for nucleotide sequencing. The sequence of various DPs was subjected to homology search by the BLAST program via the National Center

Abbreviations: AGE, advanced glycation product; AKR, aldo-keto reductase; ALR1, aldehyde reductase; ALR2, aldose reductase; DM, diabetic mouse; DP, difference product; ECM, extracellular matrix; NC, nitrocellulose; NM, normal mouse; RBG, reactive blue agarose; RDA, representational difference analysis; RSOR, renal-specific oxido-reductase.

Data deposition: The sequences reported in this paper have been deposited in the GenBank database (accession nos. AF197127, AF197128, and AF197129).

‡To whom reprint requests should be addressed at: Department of Pathology, Northwestern University Medical School, 303 East Chicago Avenue, Chicago, IL 60611. E-mail: y-kanwar@nwu.edu.

The publication costs of this article were defrayed in part by page charge payment. This article must therefore be hereby marked "*advertisement*" in accordance with 18 U.S.C. §1734 solely to indicate this fact.

Article published online before print: *Proc. Natl. Acad. Sci. USA*, 10.1073/pnas.160266197. Article and publication date are at www.pnas.org/cgi/doi/10.1073/pnas.160266197

for Biotechnology Information on-line service. The DNA fragments of the DPs that were novel and differentially regulated and had definitive mRNA transcripts by Northern blot analysis were further investigated.

cDNA Library Screening, Isolation of Full-Length cDNA, and Nucleotide Sequencing. A DP with 130 bp that yielded mRNA transcript of ≈1.5 kb was further characterized and was used for screening a mouse kidney library (13). Nitrocellulose (NC) filter lifts were made, prehybridized, and hybridized with the radiolabeled screening probe. The cDNA clones with overlapping sequences were isolated and subcloned into pBluescript II KS(+) (Stratagene), and nucleotide sequencing, homology, and protein structural analyses were performed. Rat and human kidney cDNA libraries (Stratagene) were screened to isolate mouse homologues.

Northern and Southern Blot Analyses. For Northern analyses, 30 μg of total RNAs extracted from NM and DM kidneys was glyoxylated, subjected to 1% agarose gel electrophoresis, and capillary-transferred to nylon membranes. The membrane blots were hybridized with α-^{32}P-dCTP-labeled full-length human or mouse cDNA as isolated above. The blots were washed and hybridized under high stringency conditions, and autoradiograms were prepared (13). In addition, RNAs isolated from various mouse tissues and kidneys of rat and human were processed for Northern blot analyses. For Southern blot analyses, kidney tissues from adult mouse, rat, and human were obtained, and genomic DNA was isolated (14). The DNA (10 μg) was subjected to a 0.8% agarose gel electrophoresis after digestion with various restriction endonucleases, which included *Eco*RI, *Xba*I, *Pst*I, *Bam*HI, *Hin*dIII, and *Sal*I. The gels were treated with 0.2 M HCl, followed by successive treatments with denaturing and neutralizing solutions (14). Duplicate blots were prepared by transferring the digested DNAs onto nylon membranes. The blots were hybridized either with the α-^{32}P-dCTP-radiolabeled 5′ end-specific or 3′ end-specific probes under high stringency conditions.

***In Vitro* Translation Studies.** The studies were performed to confirm the ORF of the mouse cDNA clones and to verify the size of the putative protein product. Two full-length cDNAs were selected as the template. They were subcloned into pCR2.1 vector (Invitrogen) by using PCR and sense (5′-CATGTCTTTCATTCTTTATTGATACCCAGC-3′) and antisense (5′-TTGCTCCCTCAGGATGAAGG-3′) primers. A TNT-coupled reticulocyte lysate *in vitro* translation system was used (Promega), and the translation was carried out in the presence of [^{35}S]methionine and T7 RNA polymerase. The reaction products were subjected to 10% SDS/PAGE, and autoradiograms were prepared. A positive control included luciferase-encoding plasmid that yields a translated product of ≈61 kDa.

Isolation of the Fusion Protein. Two expression constructs were generated by PCR using full-length cDNA isolated from the mouse kidney library. A *Xho*I site (**CTCGAG**) was introduced by using sense primer 5′-GGGGGG**CTCGAG**ATGAAGGTCGATGTGG-3′ and antisense primer 5′-GGGGGG**CTCGAG**TCACCAGCTCAGGGTGCCG-3′. Flanking GC clamps (GGGGGG) also were included into the primer sequences. The PCR-amplified products were digested with *Xho*I, agarose gel-purified, and ligated into the *Xho*I-digested pET-15b vector carrying an N-terminal His·Tag sequence (Novagen). The constructs were sequenced to ensure proper in-frame ligation, T*aq* polymerase fidelity, and their 5′ and 3′ end orientation. Transformation was performed by using bacterial host BL21(DE3) (Novagen). A single colony was picked, and the bacteria were allowed to grow in LB medium until an A_{600} of 0.6 was achieved. Expression of fusion proteins was induced by the addition of 1 mM isopropyl-1-thio-β-D-galactopyranoside in the medium, and the culture was extended for another 3 h. The cells were harvested by centrifugation at 5,000 × *g*, and the pellet was resuspended in an ice-cold binding buffer (5 mM imidazole/0.5 M NaCl/20 mM Tris·HCl, pH 7.9) and sonicated, and then the lysate was centrifuged at 39,000 × *g*. The supernatant was loaded onto a nickel-charged column. The column was successively washed with the binding buffer and a washing buffer (60 mM imidazole/0.5 M NaCl/20 mM Tris·Cl, pH 7.9). The bound proteins were eluted with an elution buffer (1 M imidazole/0.5 M NaCl/20 mM Tris·Cl, pH 7.9). The fractions with high content of proteins were pooled and dialyzed against 0.1 M PBS and deionized water. The purity of the isolated fusion protein was assessed by SDS/PAGE analysis.

Generation and Characterization of the Antibody. The fusion protein was used for raising polyclonal antibody in rabbits (14). For Western blot analyses, protein lysates were prepared by homogenizing various mouse tissues in ice-cold extraction buffer (10 mM Hepes/1.5 mM $MgCl_2$/10 mM KCl/0.5 mM DTT/1 mM PMSF, pH 7.4). The nuclei were pelleted by centrifuging the homogenate at 3,000 × *g* at 4°C. The concentration of the protein in the supernatant was adjusted to 20 mg/ml, followed by 10% SDS/PAGE under reducing conditions. The gel proteins were electroblotted onto a NC membrane (14). The membrane blot was immersed in a blocking solution containing 5% nonfat milk and Triton X-100 TBS (0.5% Triton X-100/0.1 M Tris/0.15 M NaCl, pH 7.5). This was followed by successive incubations, 60 min each, with the polyclonal antifusion protein antibody (1:100 dilution) and anti-rabbit IgG conjugated with horseradish peroxidase (1:1,000 dilution) at 37°C. The blot was washed three times with Triton X-100 TBS and immersed in a chemiluminescent reagent solution (Bio-Rad), and autoradiograms were developed. The analyses also were carried out on blots with the intact fusion protein and another aliquot that had been absorbed with the antibody.

Tissue Expression Studies. For *in situ* hybridization studies, the full-length cDNA clone was selected as a template to generate α-^{33}P-UTP-labeled sense and antisense riboprobes by using the Riboprobe *in vitro* Transcription System (Promega). The riboprobes then were used for *in situ* hybridization with the mouse kidney sections (13). For protein expression, 4-μm-thick cryostat kidney sections were prepared, incubated with the polyclonal antifusion protein antibody, and reincubated with goat anti-rabbit IgG antibody conjugated with FISH, and then examined with an UV light microscope. To delineate a definitive spatial distribution of the fusion protein in the kidney, its expression relative to other tubular proteins, i.e., Tamm–Horsfall protein and aquaporin-2, was investigated. Tamm–Horsfall and aquaporin-2 are markers of distal tubular and collecting duct epithelia, respectively (15, 16). Serial cryostat tissue sections were prepared and stained either with anti-Tamm–Horsfall (ICN) and antifusion protein or antiaquaporin-2 (a gift from Mark Knepper, National Institutes of Health, Bethesda, MD) and antifusion protein. The sections then were stained with secondary antibodies that were conjugated with fluorescein or rhodamine and examined.

Characterization of the Fusion Protein. Initially, immunologic cross-reactivity of the fusion protein with other enzyme proteins [aldehyde reductase (ALR1) and ALR2] that may be involved in hyperglycemic state was investigated by dot blot method. One microgram of recombinant ALR1 or ALR2 (17, 18) was applied onto a NC paper and air-dried. After blocking with 5% fat-free milk solution, the NC paper was incubated with antifusion protein antibody. The NC paper was washed with PBS contain-

ing 0.5% Tween 20 and incubated with goat anti-rabbit IgG conjugated with alkaline phosphatase. The NC paper was rewashed, and color development was performed by using AP kit (Bio-Rad). BSA was used as a negative control. A mild reactivity of the antibody with the AKR suggested that the isolated fusion protein might belong to the family of AKRs that contain NADPH-binding domain(s). This led us to investigate its affinity characteristics for NADPH by fluorescence spectrophotometry.

All fluorescence titrations were performed at 25°C in 50 mM potassium phosphate, pH 7.0 by using an excitation wavelength of 280 nm and emission wavelength of 340 nm. Various amounts of protein were titrated in 1.8 ml of assay buffer with 2- to 10-μl additions of NADPH of known concentration. A control titration without the enzyme in the same volume of buffer was carried out to correct for nonenzymatic changes in the fluorescence of NADPH. Assuming that the fluorescence quench is directly proportional to the protein–coenzyme complex, the molar fraction of the protein bound at each concentration of NADPH is given by: $\alpha = [E.\text{NADPH}]/[E]_t = F/F_{max}$, where F_{max} is the maximal fluorescence change with complete saturation, F is the observed fluorescence change and $[E]_t$ is the total protein concentration. F_{max} can be calculated from a linear double-reciprocal plot (1/fluorescence change versus1/[NADPH]) and the dissociation constant (K_d) is calculated from the replot of $1/(1 - \alpha)$ versus [NADPH]total/α according to Ward's method (19).

To confirm the NADPH binding characteristics of the fusion protein and its immunologic cross-reactivity with other reductases, i.e., ALR1 and ALR2, Western blot analyses were performed. In addition, NADPH binding characteristics of proteins present in the kidney cortex were investigated. Mouse kidney cortices were homogenized in 0.1 M potassium phosphate buffer containing 1 mM EDTA, pH 7.0. The extract was centrifuged at 13,000 $\times$ g, and the supernatant was passed through a reactive blue agarose (RBG) column (Sigma) equilibrated with the phosphate buffer. The column was washed with the same buffer and eluted with 1 mM NADPH in the buffer solution. The fractions were pooled and concentrated. Aliquots of the supernatant of the extract, eluant, fusion protein, ALR1, ALR2, and BSA were subjected to SDS/PAGE after adjusting the protein concentration. The proteins were electroblotted onto a NC membrane, and Western blotting was performed as described above by using antifusion protein antibody.

Results

Isolation and Characterization of Differentially Expressed Genes in Streptozotocin-Induced DM Kidney. Several DNAs that were differentially expressed by cDNA-RDA were identified, and one of them (130 bp) yielded a mRNA transcript of ≈1.5 kb (Fig. 1*A*) Compared with control, its expression was up-regulated in several different DM kidneys (Fig. 1*A*). The amount of total RNA loaded (30 μg) in each lane was comparable, and that is reflected in the same blot stained with methylene blue (Fig. 1*B*). The mRNA expression of β-actin was similar in DM and NM kidneys (Fig. 1*C*). Using the 130-bp DNA difference product as a screening probe, several clones were isolated. Two clones had initiation and termination codons, and they contained an ORF of 285 aa with a predicted putative protein product of ≈33 kDa. The structural analyses of the protein revealed multiple phosphorylation sites and an N-terminal AKR motif, MAKSKDSFRNYTSGPL, encompassing 21–36 amino acid residues (Fig. 1*D*). A single potential N-glycosylation site was present, and interestingly, it was located within this motif. The protein had a high aspartic acid content with a predicted pI of ≈4.88. In view of these characteristics, the protein was tentatively designated as renal-specific oxido-reductase (RSOR), although it does not have any homology with other members of the AKR family. Intriguingly, it had homologous sequences in certain segments of

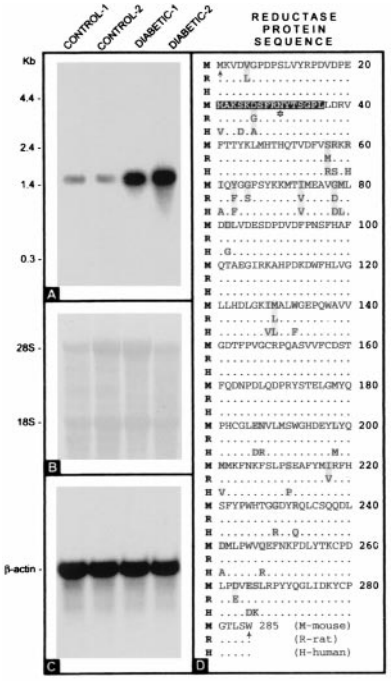

Fig. 1. (*A–C*) Northern blot analyses of RSOR in kidneys of control (NM) and DM. RSOR is up-regulated in DM kidneys (*A*). The β-actin expression is unaffected (*C*). *B* is the same blot stained with methylene blue, and it shows intactness of the RNAs and their loading of equal amounts in various lanes. (*D*) Alignment of the amino acid sequences of mouse, rat, and human RSOR. Dots indicate the identity of the amino acids. Mouse RSOR has ≈97% and ≈91% sequence homology with rat and human forms, respectively. Arrows indicate N and C terminals of the RSOR. * indicates glycosylation site. MAKSKDSFRNYTSGPL, AKR motif.

the nonmammalian proteins isolated from *Arabidopsis thaliana* and *Pinus radiata*. Among the homologues that were isolated from the cDNA libraries (Fig. 1*D*), it had ≈97% and ≈91% amino acid sequence homology with rat and human, respectively. In the mouse cDNA, an eukaryotic consensus polyadenylation site (AATAAA) was present at positions 142–147 downstream from the termination codon, suggesting that the 3′ untranslated region of the cDNA is virtually complete.

Northern Blot and Southern Blot Analyses. Using the mouse RSOR cDNA as a probe, a single mRNA transcript of ≈1.5 kb was observed in kidneys of various species (Fig. 2*A*). The blot stained with methylene blue (Fig. 2*C*) and hybridized with β-actin probe (Fig. 2*D*) indicated equal amounts of RNA loading in various lanes; however, the hybridization signal was weak in human kidney RNA. This weak signal may be caused by the use of the mouse cDNA probe and suggested that there may be differences among the various species in the genomic organization of the RSOR. This is conceivable because the blot hybridized with human RSOR cDNA as a probe revealed a relatively weak signal in mouse kidney RNA (Fig. 2*B*). Southern blot analyses yielding different banding pattern of the DNA digested with restriction endonucleases confirmed that there are significant differences in the genomic organization of the RSOR among various species (Fig. 2 *E–J*).

Verification of the RSOR cDNA and Characterization of the Fusion Protein and the Antibody. The *in vitro* translation revealed a translated product of ≈33 kDa that corresponded to the ORF of the putative protein product. Because the translated product from two different cDNA clones had identical molecular

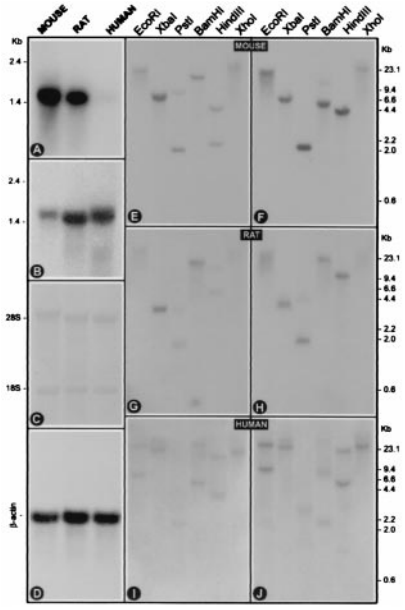

Fig. 2. (*A–D*) Northern blot of kidney mRNA of normal mouse, rat, and human, hybridized with mouse (*A*) and human (*B*) cDNA probes. A single transcript of ≈1.5 kb is observed in all of the species (*A* and *B*). Loading of equal amount of RNAs of various species is reflected by the similar intensity of 28S and 18S bands in the blot stained with methylene blue (*C*) and by comparable β-actin expression (*D*). (*E–J*) Southern blots of genomic DNA of mouse, rat, and human, digested with restriction endonucleases and hybridized with 5′ end-specific (*E, G*, and *I*) and 3′ end-specific (*F, H*, and *J*) RSOR cDNA probes. The banding profile is variable, suggesting that the genomic organization of the RSOR is different among the three species.

weights, it suggested that the isolated cDNA has a corresponding authentic protein (Fig. 3*A*). Similarly, the presence of a ≈35-kDa band in SDS/PAGE of the fusion proteins from two different clones established the authenticity of the ROSR protein (Fig. 3*B*). The excess ≈2.5-kDa mass is caused by the addition of c-*myc*-(His)6-tag. The detection of a single ≈35-kDa band by Western blot analyses confirmed identity of the protein and specificity of the polyclonal antibody (Fig. 3*C*). The specificity of the latter is further reflected by the reduction in the intensity of the band when the antibody-absorbed fusion protein was subjected to SDS/PAGE (Fig. 3*C*, lane 2).

Tissue Expression Analyses of RSOR. Northern blot analyses revealed a single ≈1.5-kb mRNA transcript in the kidney among

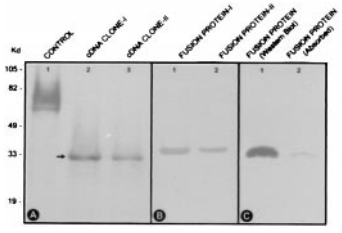

Fig. 3. (*A*) Profiles of *in vitro*-translated products. Two different cDNA clones yield identical ≈33-kDa products (lanes 2 and 3). The ≈61-kDa product in lane 1 is generated from the control plasmid. (*B*) SDS/PAGE of fusion proteins generated from two different constructs. Identical ≈35-kDa bands are seen in gel stained with Coomassie blue. Additional ≈2.5 kDa is caused by the c-*myc*-(His)6-tag in the fusion protein. (*C*) Western blot analyses of the fusion protein before (lane 1) and after (lane 2) absorption with the anti-RSOR antibody. The intensity of the ≈35-kDa band is notably reduced after absorption, suggesting that the antibody is specifically directed against the ≈35-kDa RSOR.

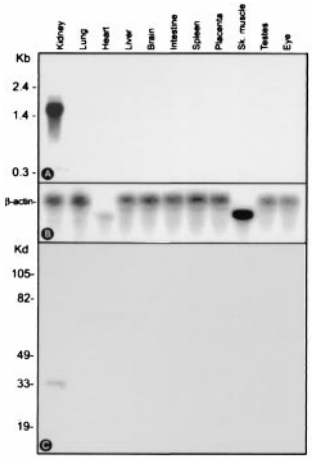

Fig. 4. (*A*) Northern blot of RNAs from various mouse tissues hybridized with RSOR cDNA. A ≈1.5-kb mRNA transcript is observed only in the kidney. The β-actin mRNA expression is similar in all of the tissues (*B*). (*C*) Western blot of protein extracts of various tissues hybridized with antifusion protein antibody. A ≈33-kDa band is seen exclusively in the kidney.

the various tissues examined (Fig. 4*A*). Similarly, Western blot analyses also indicated a single band of ≈33 kDa confined only to the kidney (Fig. 4*C*). The *in situ* tissue autoradiograms revealed that it is exclusively expressed in the tubular epithelium of the renal cortex whereas it is absent in the glomeruli and medulla (Fig. 5 *A–C*). To further delineate its expression in various renal tubular segments, immunofluorescence studies were performed on serial tissue sections stained with anti-RSOR, anti-Tamm–Horsfall, and antiaquaporin-2 antibodies. A strong intracellular immunoreactivity was seen in the tubular epithelia throughout the renal cortex of the kidney (Fig. 5 *D–F* and *J–L*). The immunoreactivity of RSOR was absent in tubular segments exhibiting immunoreactivity for Tamm–Horsfall (Fig. 5 *G–I*) and aquaporin-2 (Fig. 5 *M–O*), suggesting that the RSOR is expressed exclusively in the renal proximal tubular epithelium.

Functional Characterization of the Fusion Protein. An increasing degree of fluorescence quenching was observed with the addition of increasing amounts of NADPH, and it is graphically depicted in the titration curve (Fig. 6*A*). These results suggest that the fusion protein has a high affinity NADPH binding site or domain with $K_{\mathrm{dNADPH}} = 66.9 \pm 2.3$ nM.

The Western blot analysis, using antifusion protein antibody, also indicated the presence of such an NADPH binding protein in the kidney cortex because the eluant from the RBG column yielded a band of ≈33 kDa (Fig. 6*B*, lane 4). The immunoreactivity of the band was less compared with the whole homogenate of the kidney cortex (Fig. 6*B*, lane 3), although comparable amounts of protein were loaded for SDS/PAGE analyses. It is conceivable that exact protein concentration may be difficult to assess by the Bio-Rad protein assay in the eluant from the RBG column because protein is still bound to the NADPH. The fusion protein band was ≈35 kDa, where ≈2.5 kDa is caused by the presence of c-*myc*-(HIS)6-tag (Fig. 6*B*, lane 5). No immunoreactivity with the BSA (Fig. 6*B*, lane 6) and negligible reactivity with the recombinant ALR2 (Fig. 6*B*, lane 2) were observed. Interestingly, a mild immunoreactivity was detected with the recombinant ALR1 (Fig. 6*B*, lane 1), suggesting that polyclonal antifusion antibody has some cross-reactivity with other members of the AKR family. By densitometric analysis, the intensity of the recombinant ALR1 band was ≈25-fold less compared with the novel fusion protein (Fig. 6*B*, lane 1 vs. 5).

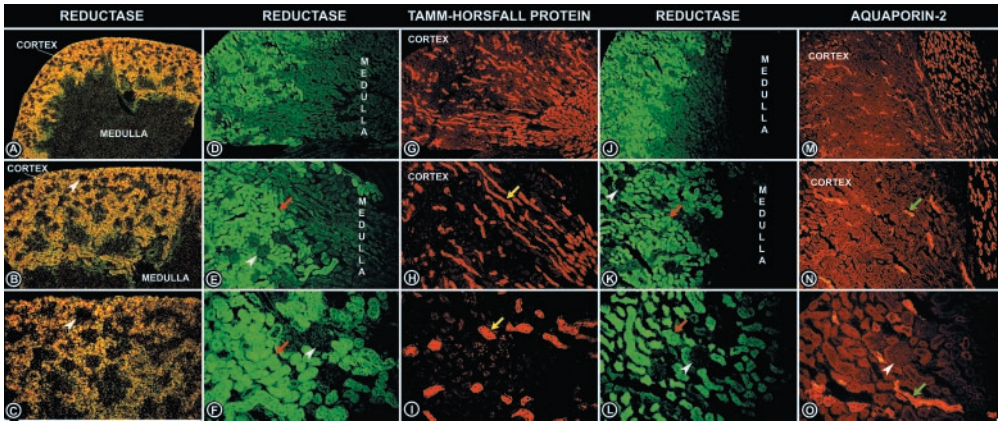

Fig. 5. Low (*A*), medium (*B*), and high (*C*) magnification photomicrographs of *in situ* autoradiograms of kidney tissue sections hybridized with RSOR riboprobe. The RSOR mRNA is exclusively expressed in tubules of the renal cortex and is absent in the medulla and glomeruli (arrowheads). (*D–F* and *J–L*) Photomicrographs with different magnifications of the kidney sections stained with anti-RSOR antibody. The spatial protein expression of RSOR is similar to the mRNA message, and it is absent in the medulla and glomeruli (arrowheads). (*G–I*) Immunofluorescence photographs of kidney sections stained with anti-Tamm–Horsfall protein antibody, a marker of distal tubular epithelium (arrows). The photographs depicted in *G–I* are the serial tissue sections of micrographs shown in *D–F*. (*M–O*) Immunofluorescence photographs of kidney sections stained with anti-aquaporin-2 antibody, a marker of collecting duct epithelium (arrows). The photographs depicted in *M–O* are the serial tissue sections of micrographs shown in *J–L*. Absence of RSOR immunoreactivity in the distal and collecting tubules suggests that it is exclusively expressed in the proximal tubules. Magnifications: *A*, *D*, *G*, *J*, and *M*, ×10; *B*, *E*, *H*, *K*, and *N*, ×20; *C*, *F*, *I*, *L*, and *O*, ×40.

Discussion

AKRs are a family of monomeric oxido-reductases that catalyze the NADPH-dependent reduction of a wide variety of aliphatic and aromatic aldehydes and ketones (11). The functions of most of the family members are not very well defined, nevertheless, ALR1 and ALR2 have been under intense investigation (7, 10, 17, 20–25), and the latter has received the most attention because of its pathophysiologic relevance to diabetic complications (26). Besides, the increased amounts of glycated proteins and sorbitol, the ALR2 activity and expression of its ≈1.5-kb mRNA transcript have been found to be up-regulated in kidneys of diabetic rats (27, 28). Because a similar-sized mRNA transcript was found to be up-regulated in several DM kidneys, our initial considerations were that the 130-bp clone isolated by cDNA-RDA is a fragment of the known mammalian ALR2. However, the fact that no sequence homology was observed led us to isolate the full-length cDNA. The latter, with a putative protein product of ≈33 kDa, also did not reveal any sequence homology with AKR family members or other known mammalian sequences in the GenBank database. However, the isolated cDNA had partial homology with proteins derived from *A. thaliana* and *P. radiata*. The fact that rat and human cDNA sequences were quite homologous and yielded similar ORFs and mRNA transcripts indicated that it is likely a translatable gene. Such a notion was supported by *in vitro* translational studies where identical molecular weight bands were observed by using two different cDNA clones. Similarly, generation of identically sized recombinant proteins from different cDNA clones further supports the translatability of the isolated cDNA.

Unlike the ALR1 and ALR2 that are widely distributed in various tissues, the mRNA transcript of the isolated clone was exclusively expressed in the kidney. Both ALR1 and ALR2 and AKR-related family members have been isolated from the kidney, but their sequences are nonhomologous with this renal-specific cDNA (29, 30). The Western blot, using antifusion protein antibody, confirmed that it is exclusively expressed in the kidney. Next, intrarenal spatial distribution of this renal-specific gene was studied in view of the fact that ALRs also are expressed in the kidney (30). The ALR2 is expressed in the mesangial cells where it is involved in the pathophysiology of the glomerulus in diabetes (31), and it is also present in the medulla where it is believed to serve as an osmolyte regulator (32). Unlike the ALRs, both mRNA and protein expression of this novel gene were confined to the cortical tubules and not in the glomeruli. Further delineation of its expression revealed that it neither codistributes with Tamm–Horsfall protein nor with aquaporin-2, indicating that it is restricted to the proximal tubular epithelia, and thus can be regarded as one of their specific markers. In addition, immunofluorescence studies suggest that it is an intracytoplasmic protein, and that is in line with its deduced

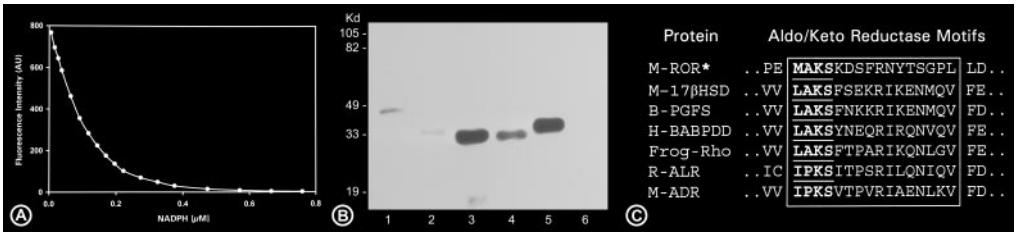

Fig. 6. (*A*) Titration curve depicting a high affinity of the RSOR fusion protein for NADPH. (*B*) SDS/PAGE of various proteins analyzed by Western blot hybridized with antifusion protein antibody. Lane 1, ALR1; lane 2, ALR2; lane 3, kidney cortex extract; lane 4, RBG column eluant of the kidney extract, lane 5, RSOR fusion protein; lane 6, BSA. Reactivity with the eluant from RBG column (lane 4) indicates recognition of NADPH binding protein by the anti-RSOR antibody. Mild cross-reactivity with the ALR1 also is observed (lane 1). (*C*) Comparison of amino acid sequence of AKR motifs. Motif sequences are boxed. The NADPH binding sites are bolded and underscored. M-RSOR*, mouse RSOR; M-17βHSD, mouse 17β-hydroxysteroid dehydrogenase; B-PGFS, bovine lung prostaglandin F synthase; H-BABPDD, bile acid binding protein dihydrodiol dehydrogenase; Frog-Rho, ρ-crystallin; R-ALR1, rat ALR1; M-ALR2, mouse ALR2.

protein sequence where no extended transmembrane hydrophobic stretches were observed.

Interestingly, a stretch of amino acids identified as AKR-3 signature was observed in this renal proximal tubular epithelial-specific protein. The fact that its molecular weight was comparable to most of the AKR members, i.e., 30–40 kDa, and being acidic, i.e., pI ≈4.9, suggested that it may have properties that are characteristic of this superfamily. Fluorescence quenching studies indeed indicated that it has a high affinity binding site for NADPH with $K_{dNADPH} = \approx 67$ nM. The Western blotting of the eluant proteins from the RBG column also attests that it is a NADPH binding protein and can be designated as RSOR. The NADPH binding site is located within the AKR-3 motif, and a comparison of this domain with other AKR members is shown in Fig. 6*C*. It is conceivable that because of the sequence similarity in AKR motif and NADPH domain a weak RSOR-antibody cross-reactivity with the ALR2 was observed. The domain is comprised of a tetrapeptide, Ile-Pro-Lys-Ser (IPKS), where the first two amino acids may be variable. The lysine residue seems to be the critical amino acid residue because its modification by pyridoxal 5′ phosphate affects the catalytic efficiency of ALR1 and ALR2 (21, 23). Intriguingly, the AKR-3 motif in the RSOR is located near the N terminus, whereas it is confined to the C terminus in most of the AKR members, including some of the structural proteins, e.g., ρ-crystallin (33). The significance of the C terminus, in terms of substrate binding sites of the ALRs, is emphasized by studies where substitution or mutation of amino acids downstream of the AKR-3 motif, i.e., Arg^{311} in ALR1, and Cys^{298} and Cys^{303} in ALR2, resulted in their altered catalytic properties (17, 24, 34). Such studies are deemed necessary to determine the kinetic properties and substrate specificity of the RSOR. Initial attempts to study the kinetic properties of RSOR, using traditional substrates, e.g., D-glucose and DL-glyceraldehyde, were not successful. It may be that the AKR-3 motif is located near the N terminus and contains an N-linked glycosylation site. The latter may be needed for the catalytic activity of RSOR, although it seems not to be essential for the activity of ALR1 or ALR2, in which the AKR-3 motif is not glycosylated. Certainly, studies are anticipated in which RSOR would be expressed in insect cells to isolate its glycosylated form for the delineation of its substrate specificity, catalytic domains, and kinetic properties.

In summary, a RSOR with high affinity for NADPH that is up-regulated in experimental streptozotocin-induced diabetes mellitus is described, and the mechanism(s) by which its expression is modulated by hyperglycemia, whether related to the oxidant or osmotic stress, should be the subject of further studies. Finally, because the RSOR's expression is tubular-specific, the studies also would yield important clues as to the pathogenesis of tubular lesions, which incidentally also play a major role in the pathogenesis of renal complications in diabetes mellitus (35).

This work was supported by National Institutes of Health Grants DK28492 and DK36118.

1. Parving, H.-H., Osterby, R. & Ritz, E. (2000) in *The Kidney,* ed. Brenner, B. M. (Saunders, Philadelphia), pp. 1731–1773.
2. Sharma, K. & Ziyadeh, F. N. (1994) *Am. J. Physiol.* **266,** F829–F842.
3. Border, W. A. (1994) *Curr. Opin. Nephrol. Hypertens.* **3,** 54–58.
4. Khalifah, R. G., Baynes, J. W. & Hudson, B. G. (1999) *Biochem. Biophys. Res. Commun.* **257,** 251–258.
5. Casey, E. B., Zhao, H.-R. & Abraham, E. C. (1995) *J. Biol. Chem.* **270,** 20781–20786.
6. Zhao, H.-R., Nagaraj, R. H. & Abraham, E. C. (1997) *J. Biol. Chem.* **272,** 14465–14469.
7. Gabbay, K. H., Merola, L. O. & Field, R. A. (1966) *Science* **151,** 209–210.
8. Bleyer, A. J., Fumo, P., Snipes, E. R., Goldfarb, S., Simmons, D. A. & Ziyadeh, F. N. (1994) *Kidney Int.* **45,** 659–666.
9. Morrisey, K., Steadman, R., Williams, J. D. & Phillips, A. O. (1999) *Kidney Int.* **55,** 160–167.
10. Vander Jagt, D. L., Robinson, B., Taylor, K. K. & Hunsaker, L. A. (1992) *J. Biol. Chem.* **267,** 4364–4369.
11. Jez, J. M., Flynn, T. G. & Penning, T. M. (1997) *Biochem. Pharmacol.* **54,** 639–647.
12. Wada, J. & Kanwar, Y. S. (1998) *Proc. Natl. Acad. Sci. USA* **95,** 144–149.
13. Wada, J., Kumar, A., Liu, Z., Ruoslahti, E., Reichardt, L., Marvaldi, J. & Kanwar, Y. S. (1996) *J. Cell Biol.* **132,** 1161–1176.
14. Wada, J. & Kanwar, Y. S. (1997) *J. Biol. Chem.* **272,** 6078–6086.
15. Venkatachalam, M. A. & Kriz, W. (1992) in *Pathology of the Kidney*, ed. Heptinstall, R. H. (Little, Brown, Boston), pp. 1–90.
16. Knepper, M. A., Verbalis, J. G. & Nielson, S. (1997) *Curr. Opin. Nephrol. Hypertens.* **6,** 367–371.
17. Petrash, J. M., Harter, T. M., Devine, C. S., Olins, P. O., Bhatnagar, A., Liu, S. & Srivastava, S. K. (1992) *J. Biol. Chem.* **267,** 24833–24840.
18. Das, B. & Srivastava, S. K. (1985) *Biochim. Biophys. Acta* **840,** 324–333.
19. Ward, L. K. (1985) *Methods Enzymol.* **117,** 400–414.
20. Bohren, K. M., Bullock, B., Wermuth, B. & Gabbay, K. H. (1989) *J. Biol. Chem.* **264,** 9547–9551.
21. Morjana, N. M., Lyons, C. & Flynn, T. G. (1989) *J. Biol. Chem.* **264,** 2912–2919.
22. Vander Jagt, D. L., Robinson, B., Kelly, K. T. & Hunsaker, L. A. (1990) *J. Biol. Chem.* **265,** 20982–20987.
23. Flynn, T. G., Lyons, C. & Hyndman, D. J. (1990) *Adv. Enzymol.* **30,** 195–213.
24. Bohren, K. M., Grimshaw, C. E. & Gabbay, K. H. (1992) *J. Biol. Chem.* **267,** 20965–20970.
25. Liu, S. Q., Bhatnagar, A. & Srivastava, S. K. (1993) *J. Biol. Chem.* **268,** 25494–25499.
26. Fuji, J., Takahashi, M., Hamaoka, R., Kawasaki, Y., Miyazawa, N. & Taniguchi, N. (1999) *Adv. Exp. Med. Biol.* **463,** 419–426.
27. Das, B. & Srivastava, S. K. (1985) *Diabetes* **34,** 1145–1151.
28. Ghahary, A., Luo, J., Gong, Y., Chakrabarti, S., Sima, A. A. F. & Murphy, L. J. (1989) *Diabetes* **38,** 1067–1071.
29. Gui, T., Tanimoto, T., Kokai, Y. & Nishimura, C. (1995) *Eur. J. Biochem.* **277,** 448–453.
30. Robinson, B., Hunsaker, L. A., Strangebye, L. A. & Vander Jagt, D. L. (1993) *Biochim. Biophys. Acta* **1203,** 260–266.
31. Kikkawa, R., Umemura, K., Haneda, M., Kajiwara, N., Naeda, S., Nishimura, C. & Shigeta, Y. (1992) *Diabetes* **41,** 1165–1171.
32. Schwartz, G. J., Zavilowitz, B. J., Radice, A. D., Garcia-Perez, A. & Sands, J. M. (1992) *J. Clin. Invest.* **90,** 1275–1283.
33. Carper, D., Nishimura, C., Shinohara, T., Dietzchold, B., Wistow, G., Craft, C., Kador, P. & Kinoshita, J. H. (1987) *FEBS Lett.* **220,** 209–213.
34. Barski, O. A., Gabbay, K. H. & Bohren, K. M. (1996) *Biochemistry* **35,** 14276–14280.
35. Ihm, C. G., Lee, G. S. L., Nast, C. C., Artishevsky, A., Guillermo, R., Levin, P. S., Glassock, R. J. & Adler, S. G. (1992) *Kidney Int.* **41,** 768–777.